HHS Public Access

Author manuscript

*Clin Cancer Res*. Author manuscript; available in PMC 2017 January 12.

Published in final edited form as:

*Clin Cancer Res*. 2014 December 15; 20(24): 6389–6397. doi:10.1158/1078-0432.CCR-14-1524.

# In-vivo quantification of hypoxic and metabolic status of NSCLC tumors using [$^{18}$F]HX4 and [$^{18}$F]FDG PET/CT imaging

**Catharina M.L. Zegers**[1], **Wouter van Elmpt**[1], **Bart Reymen**[1], **Aniek J.G. Even**[1], **Esther G.C. Troost**[1], **Michel C. Öllers**[1], **Frank J.P. Hoebers**[1], **Ruud M.A. Houben**[1], **Jonas Eriksson**[2], **Albert D. Windhorst**[2], **Felix M. Mottaghy**[3,4], **Dirk De Ruysscher**[1,5], and **Philippe Lambin**[1]

[1]Department of Radiation Oncology (MAASTRO), GROW - School for Oncology and Developmental Biology, Maastricht University Medical Centre, Maastricht, The Netherlands [2]Department of Radiology &Nuclear Medicine, VU University Medical Centre, Amsterdam, The Netherlands [3]Department of Nuclear Medicine, Maastricht University Medical Centre, Maastricht, The Netherlands [4]Department of Nuclear Medicine, University Hospital Aachen, Germany [5]University Hospitals Leuven/ KU Leuven, Leuven, Belgium

## Abstract

**Objective—**Increased tumor metabolism and hypoxia are related to poor prognosis in solid tumors, including non-small cell lung cancer (NSCLC). PET imaging is a non-invasive technique which is frequently used to visualize and quantify tumor metabolism and hypoxia. The aim of this study was to perform an extensive comparison of tumor metabolism using FDG PET and hypoxia using HX4 PET imaging.

**Materials/Methods—**FDG- and HX4-PET/CT images of 25 NSCLC patients were co-registered. At a global tumor-level, HX4 and FDG parameters were extracted from the gross-tumor-volume. The HX4-high fraction and high volume were defined using a tumor-to-blood ratio>1.4. For FDG-high fraction and high volume a SUV>50% of $SUV_{max}$ was used. We evaluated the spatial correlation between HX4 and FDG uptake within the tumor, to quantify the (mis)match between volumes with a high FDG and high HX4 uptake.

**Results—**At a tumor-level, significant correlations were observed between FDG and HX4 parameters. For the primary GTV, the HX4-high fraction was three times smaller compared to the FDG-high fraction. In 53% of the primary lesions, less than 1$cm^3$ of the HX4-high-volume was outside the FDG-high volume; for 37% this volume was 1.9–12$cm^3$. Remarkably, a distinct uptake pattern was observed in 11%, with large hypoxic volumes localized outside the FDG-high volume.

**Conclusion—**Hypoxic tumor volumes are smaller than metabolic active volumes. Approximately half of the lesions showed a good spatial correlation between the PET tracers. In the other cases, a (partial)mismatch was observed. The addition of HX4-PET imaging has the potential to individualize patient treatment.

Corresponding author: Catharina M.L. Zegers, Maastro Clinic, Dr. Tanslaan 12, 6229ET Maastricht, The Netherlands, Phone: +31884455666, Fax: +31884455667, karen.zegers@maastro.nl.

**Conflicts of interest:** No actual or potential conflicts of interest exist.

**Keywords**

NSCLC; hypoxia; PET; HX4; FDG

## Introduction

Lung cancer has the highest death rate among leading cancer types (1). Standard treatment for advanced stage non-small cell lung cancer (NSCLC) is the combination of radiotherapy (RT) and chemotherapy, administered either sequentially or concurrently (2). Tumor cell hypoxia has a negative impact on cancer treatment effectiveness, it promotes resistance to radiotherapy (RT) and chemotherapy, increases the metastatic potential, and is therefore related to a poor prognosis (3–5). Tumor hypoxia is present in the majority of NSCLCs, which can be visualized and quantified using functional PET imaging with radiolabeled 2-nitroimidazoles (6, 7).

3-[$^{18}$F]fluoro-2-(4-((2-nitro-1*H*-imidazol-1-yl)methyl)-1*H*-1,2,3-triazol-1-yl)propan-1-ol ([$^{18}$F]HX4) is a relatively new nitroimidazole with attractive pharmacokinetic properties that has successfully completed preclinical and clinical testing (8–10).

In standard clinical practice, a combination of anatomic computed tomography (CT) and functional [$^{18}$F]fluorodeoxyglucose (FDG) PET imaging is frequently used to visualize, detect and stage malignancies. In addition, FDG PET can be used to identify subvolumes with a high metabolism, which are more susceptible to local recurrence after (chemo)radiotherapy (11, 12). Aerts et al. showed that the residual tumor volume after RT is mainly located within the pre-RT high FDG-uptake volume. However, 30% of the residual volume did not correspond to the high FDG volume (11, 13). This may be caused by tumor regrowth in pre-RT hypoxic tumor subvolumes located outside the high FDG volume. Therefore, it is of great interest to investigate the correlation between both unfavorable biological features (high tumor metabolism, hypoxia) since they can be used to predict treatment outcome. In addition, imaging-derived tumor features have the potential to guide treatment with hypoxic modifiers or radiotherapy dose-painting (14–16). The uptake of FDG in the cell is dependent on the over-expression of glucose transporters (GLUT), which can be upregulated in the absence of oxygen, through the HIF1α-mediated pathway (17). This may suggest a possible overlap between volumes of high FDG uptake and tumor hypoxia, even though they represent different biological properties of tumors.

The aim of this study was to perform an extensive comparison of tumor metabolism, using FDG, and hypoxia, using HX4, to fully characterize the relationship between both PET tracers on a global tumor and voxel level for primary NSCLC and the regional lymph node metastases.

## Materials and Methods

### Patients

FDG and HX4 PET/CT images of 25 NSCLC patients (17 male, 8 female) were acquired before the start of external beam radiotherapy. The average age of the patients was 63y

(range 40–82y). Tumor stage ranged from IIB-IV, pathology being adenocarcinoma (N=13), squamous cell carcinoma (N=5), large cell carcinoma (N=7). Patients were treated with radical radiotherapy (N=3) or chemo-radiation (N=22), with the majority of patients receiving at least one cycle of chemotherapy before PET imaging and before the start of radiotherapy (Supplementary Table S1). PET data were acquired in the translational research part of two phase II trials [PET-Boost, NCT01024829 (18); Nitroglycerin (NCT01210378)], both having identical PET imaging procedures. The clinical trials were approved by the appropriate medical ethical review committee, and all patients provided written informed consent before study entry.

## PET/CT imaging

HX4 was produced as described in previous publications (8–10, 19). After intravenous administration of 429±57 MBq HX4, PET/CT imaging was performed at 4h post-injection (p.i.) for 20–30 minutes in a single bed position centered around the primary tumor. HX4 PET/CT images were acquired on a Gemini TF 64 scanner (Philips Healthcare, Best, the Netherlands), with a spatial resolution of approximately 5 mm FWHM. We performed CT-based attenuation correction and scatter correction (SS-SIMUL), and reconstructed PET images using 3D ordered subset iterative time-of-flight reconstruction technique (BLOB-OS-TF) with 3 iterations and 33 subsets in a 144 × 144 matrix and voxel sizes of 4 × 4 mm.

The injected activity of FDG depended on the patient's weight according to the national guidelines (20). PET/CT imaging was performed one hour after intravenous administration of FDG. FDG PET/CT scans were acquired using a Biograph 40 PET/CT scanner (Siemens Healthcare, Erlangen, Germany); scatter and attenuation correction were applied; and PET images were reconstructed using OSEM 2D (Ordered Subset Expectation Maximization, 4 iterations, 8 subsets) and a Gaussian filter of 5 mm. A respiratory correlated CT was performed, with the mid-ventilation scan selected for the attenuation correction and fusion with the FDG PET.

HX4 and FDG PET/CT scans were acquired in the same week for all except one patient. The median interval between both PET scans was 3 days (range: 1–14d). No interventions (e.g. radiotherapy or chemotherapy) were performed between the FDG and HX4 PET scans. Both scans were acquired with the patient positioned in radiotherapy position, on a flat tabletop using a laser alignment system with arms in an arm-support positioned above the head.

## Analysis

For all patients, gross tumor volumes (GTVs), including the primary lesion (GTVprim) and involved lymph nodes (GTVln), were defined on the FDG PET/CT scan by two experienced radiation oncologists in consensus. GTVprim and GTVln were analyzed separately. Lesions with a size <5 $cm^3$ were excluded due to potential partial volume effects.

The FDG PET/CT was rigidly registered to the HX4 PET/CT using registration software developed in-house. The rigid transformation was determined by the registration of the FDG-CT to the HX4-CT; the same transformation was subsequently applied to the FDG PET scan and the GTVs. A volume of interest in the aorta was defined as background region.

The maximum and mean standardized uptake values ($SUV_{max}$ and $SUV_{mean}$), corrected for body weight, were determined within the GTV for both FDG and HX4 PET. For the HX4 PET, calculations were made of the maximum tumor-to-blood ratio ($TBR_{max}$), defined as the $SUV_{max}$ in the tumor divided by the $SUV_{mean}$ in the aorta, the HX4 high-fraction (HX4-HF) and HX4 high-volume (HX4-HV), both defined as the fraction/volume of the GTV with a TBR>1.4. For the FDG PET, calculations were made of the FDG high-fraction (FDG-HF) and FDG high-volume (FDG-HV) based on the PET-Boost trial strategy, using the GTV volume with an SUV above 50% of the $SUV_{max}$ (18).

This classification for defining HX4 high and FDG high volumes, as a fraction of the total GTV, was used to sub-divide regions of a tumor into four classes: (i) FDG low and HX4 low, (ii) FDG high and HX4 low, (iii) FDG low and HX4 high, and (iv) FDG high and HX4 high. To evaluate the effect of the threshold definition on tumor sub-division, a calculation was made of the average distribution using alternative thresholds. The HX4 threshold varied from TBR>1.3 to TBR>1.5; the FDG threshold ranged from SUV>30 to SUV>70% of $SUV_{max}$.

A visual and voxel-wise comparison of the FDG and HX4 uptake within the GTV was performed to compare spatial uptake patterns in the primary lesions. Based on the voxel-wise analysis we separated lesions into three groups. First, in lesions showing a high correlation between the FDG and HX4 uptake, the hypoxic volume was entirely within the high metabolic volume. Second, in lesions showing a moderate correlation between the FDG and HX4 uptake, there was only a partial overlap between the HX4-HV and the FDG-HV. Third, in lesions showing a different uptake pattern between the two tracers, there were two distinct regions of FDG-HV and HX4-HV.

### Statistics

Mean ± 1 standard deviation (SD) were reported for all parameters. Linear and multiple linear regressions were performed to correlate the GTV based parameters ($SUV_{max}$, $SUV_{mean}$, TBR, HF, HV) and to quantify the voxel-wise comparison of the FDG and HX4 uptake. Pearson correlation coefficients were calculated. A p-value $<0.05$ was assumed to be statistically significant.

## Results

### Overall correlation of FDG and HX4 parameters

This study analyzed the overall FDG and HX4 uptake in the primary tumor and lymph nodes of 25 NSCLC patients. All GTVprim (N=25) and 19 GTVln were larger than 5 $cm^3$ and all were used for the analysis. The average values of the GTV, FDG and HX4 parameters are shown in Table 1. The sub-classification, based on tumor pathology, showed no significant differences for any of the FDG or HX4 parameters (examples are shown in supplementary Figure S1). The FDG-HV was larger than the HX4-HV in 24/25 GTVprim and in all GTVln. Potential correlations between FDG and HX4 PET based parameters were investigated.

The correlation coefficients for the *primary tumors* are shown in Table 2. The majority of the FDG and HX4 PET based parameters showed a significant correlation with the primary

tumour volume. Note that the HX4-HV was significantly correlated with the tumor volume, while the HX4-HF was not. The FDG-$SUV_{mean}$ correlated positively with all HX4 PET parameters. The FDG-$SUV_{max}$ only showed a significant correlation with HX4-$SUV_{max}$ (R=0.54 p<0.01), HX4-TBR (R=0.55, $p$<0.01) and HX4-HV (R=0.66, $p$<0.001). The highest correlations were observed when comparing the FDG-HV with the HX4 based parameters: HX4-$SUV_{max}$ (R=0.63, $p$<0.01), HX4-TBR (R=0.62, $p$<0.01), and HX4-HV (R=0.76, $p$<0.0001). Two examples are shown in Figure 1. From Figure 1B one can appreciate that, although there is a correlation between FDG-$SUV_{max}$ and HX4-$TBR_{max,}$ it is not possible to distinguish the non-hypoxic lesions by using only the FDG-$SUV_{max}$ parameter.

A multiple linear regression was performed in order to test the interaction between primary tumour volume and FDG parameters to predict the hypoxic volume. Using the parameters primary tumor volume and FDG-$SUV_{max}$ to predict HX4-HV, we observed a correlation coefficient of 0.74 ($R^2$= 0.55) with a significant contribution of both FDG-$SUV_{max}$ (p<0.01) and primary tumor volume (p=0.03). Adding the interaction term (FDG-$SUV_{max}$ *primary tumor volume) to the model increases the correlation coefficient to 0.82 ($R^2$=0.67).

For the *involved lymph nodes* GTVln volume has a large effect on the correlation coefficients between the HX4 and FDG parameters (Supplementary Table 2). The multiple linear regression using GTVln volume and FDG-$SUV_{max}$ to predict HX4-HV (R=0.96) therefore only showed a significant contribution for the GTVln volume (p<0.001) and not for FDG-$SUV_{max}$ (p=0.26).

### Average distribution of FDG and HX4 uptake

The average distribution within the primary tumor based on the four previously predefined categories is shown in Table 3 and visualized in Figure 2A. On average, the FDG high volume is 42±21% of the GTVprim, of which 10±12% is hypoxic. On average, 3% (range: 0–31%) of the GTVprim is hypoxic but outside the FDG-HV, representing 24% (3.2%/ 13.6%) of the total hypoxic volume.

The effect of alternative thresholds on the average distribution of FDG and HX4 within the primary tumor is shown in Supplementary Table S3 and visualized for two examples in figures 2B and 2C. This figure shows that the hypoxic percentage of the GTV (HX4-HF) outside the high FDG area (FDG-HF) is relatively stable.

### Spatial correlation of FDG and HX4 uptake patterns

Tracer uptake above the background level in both PET scans is essential for comparing the overlap of FDG and HX4 high volumes. All primary lesions showed FDG uptake with an $SUV_{max}$>3.5, however, only 19 out of 25 primary lesions expressed an HX4 uptake (TBR > 1.4). These 19 lesions were selected for further analysis.

Based on the voxel-wise analysis we observed that in 10 lesions, less than 1 $cm^3$ of the HX4-HV was outside the FDG-HV (group 1, Figure 3A). In 7 lesions, 2–12 $cm^3$ of the HX4-HV was outside the FDG-HV (group 2, Figure 3B). Finally, in 2 patients a clearly distinct uptake pattern was observed between the two tracers and hypoxic volumes of 46

$cm^3$ and 102 $cm^3$ were observed outside the FDG high uptake region, which were 73% and 78% of the total HX4-HF, respectively (group 3, Figure 3C). The primary tumor volume was significantly correlated to the group the lesion was assigned to ($R=0.75$; $p<0.01$).

## Discussion

This study was initiated to assess the correlation of (spatial) uptake patterns of hypoxia (using HX4 PET) and tumor metabolism (using FDG PET) in primary NSCLC and associated lymph node metastases. Both biological features are known to have an adverse impact on treatment outcome in NSCLC. FDG PET is routinely used in clinical practice for staging, radiotherapy planning and treatment response monitoring, while the use of hypoxia (HX4) PET imaging is still limited to clinical trials. We show in 25 NSCLC patients, with different histopathological subtypes, that HX4 PET imaging provides additional information to FDG PET which can be used to individualize patient treatment.

The relationship between HX4 and FDG PET was investigated at a tumor level by comparing the overall uptake within the GTVs of the primary tumor and lymph node metastases. Significant correlations were observed between GTV, HX4 and FDG PET image parameters. Previous studies comparing the overall uptake of hypoxia PET and FDG PET showed varying results. No correlations were observed by Bollineni et al. (7) or Cherk et al. (21), while Vera et al. (22) reported a significant correlation. Gagel et al. (23) compared FDG and FMISO uptake to the gold standard of hypoxia measurements ($pO_2$ polarography) and observed a moderate correlation for FMISO but no correlation for FDG. However, since both FDG-$SUV_{max}$ and GTV volume are predictors of survival in NSCLC (24–26) and the amount of tumor hypoxia is related to outcome after radiotherapy (27), the reported correlation between hypoxia and FDG PET is plausible.

Information about hypoxia on a tumor level can be used in clinical practice to select patients who may benefit from hypoxia modification before or during anti-cancer treatment. Previous studies have shown that the addition of hypoxic modification during radiotherapy results in an increased therapeutic benefit (28). Recently, Arrieta et al. (29) investigated in NSCLC patients the use of nitroglycerin (an organic nitrate which causes vasodilatation, increased blow flow and reduces the expression of HIF1-α) in combination with chemo-radiation. In this study promising response rates were observed, however, there was also (mild) increased toxicity (e.g. headache, hypotension) due to nitroglycerin administration. Another promising compound is the hypoxia activated prodrug TH-302 which releases bromo isophosphoramide mustard, a potent DNA alkylating agent, in hypoxic regions. Saggar et al. (30) recently demonstrated that TH-302 administered togheter with chemotherapy enhances the anti-tumor effect but also increases toxicity. From these recent studies we acknowledge the therapeutic effect of additional anti-hypoxia treatment, but also the importance to limit unnecessary toxicity by selecting patients who will benefit from these modifications. We show that we can non-invasively visualize and quantify tumor hypoxia, using HX4 PET, in patients with NSLSC. In addition, our results show that patients with a larger tumor size and higher FDG uptake are more likely to have a larger hypoxic volume. This combination (GTV size and FDG uptake) could be used as a surrogate for hypoxia PET imaging, however, despite the correlation between hypoxia and FDG parameters, the distinction

between hypoxic and non-hypoxic tumors based on FDG PET can be misleading, since non-hypoxic tumors are present in a broad range of FDG uptake (FDG-$SUV_{max}$: 3.5 – 17.5 also shown in Figure 1B).

It is important to note that a correlation at a global tumor level provides no information about the intratumoral heterogeneity. At the moment, limited data is available concerning the correlation of hypoxia PET and FDG PET at a subvolume (e.g. voxel) level in NSCLC (7, 31). The spatial concordance and discordance of both PET modalities is of interest for radiotherapy boosting strategies. FDG PET is already used in the context of clinical trials to boost highly metabolic tumor subvolumes (18, 32). We hypothesize that hypoxia PET imaging may be more selective in defining radioresistant voxels within the GTV, and can provide complementary information regarding the definition of radiotherapy boost volumes. A voxel-wise comparison was performed to evaluate the spatial distribution of the HX4 and FDG uptake. A reasonable correlation between both tracers was observed in the majority of patients. This is in contradiction to the previous published results of Bollineni et al. (7), who observed no correlation between FDG and the hypoxia PET tracer FAZA. This disagreement can probably be explained by the definition of the target lesion. Bollineni et al. used an FDG based threshold to define the target lesion, thereby excluding voxels with a low FDG uptake. Conversely, Lohith et al. (31) reported a similar spatial distribution of [$^{62}$Cu]ATSM and FDG in 5 patients with an adenocarcinoma of the lung, which was not present in squamous cell carcinomas (SCC) patients. Also, they observed a difference in intra-tumoral distribution between adenocarcinoma and SCC, which was not observed in our cohort of NSCLC patients. It is well described that hypoxia leads to an increased uptake of glucose through various molecular mechanisms (33). Nevertheless, an increased glycolysis is also observed without hypoxia, e.g. by c-myc aberrations (34). From a molecular point of view, it is therefore logical that FDG uptake and hypoxia is partially overlapping and is highly dependent on the genetics of the tumour.

Thresholds were defined arbitrarily to define regions with a high or low uptake on both FDG and HX4 PET. The high FDG PET volume was defined based on the ongoing NSCLC boost trial (18), whereas the high HX4 region was based on previous publications, indicating that a threshold of TBR>1.4 is rational to define hypoxia (6, 8, 35, 36). These thresholds showed the HX4 high volume to be three times smaller on average than the FDG high volume.

This work can be used in clinical setting to divide patients with a hypoxic lesion into different groups, stratifying lesions with an agreement or disagreement between the HX4 and FDG PET uptake pattern. In the patients with an concordance, the use of HX4 PET has limited additional value for the selection of the radiotherapy boost volume, however, this volume could be limited to HX4 high areas only, facilitating further dose escalation without comprising the surrounding healthy tissue. In other patients a (partial) discordance between the HX4 and FDG PET uptake pattern was observed. In these patients, the boost region could be adjusted to either HX4 PET or a combination of HX4 and FDG PET with the aim to improve loco-regional control. Based on the current analysis, a radiation boost to the FDG high area (SUV>50% $SUV_{max}$) would on average miss 24% of the hypoxic volume, which seems in agreement with the residual activity after RT outside the high-FDG area as reported by Aerts et al. (11). Previous studies have already shown that radiotherapy dose distribution

based on tumor hypoxia is possible and promising (37, 38). Currently there are strategies available to investigate the original location of local recurrences inside the tumor volume (39). These studies will characterize the subvolumes inside the heteregenous tumour that are difficult to control. Ultimately, the effect of tumour subvolume characterization and targeting, by radiotherapy or other therapeutic interventions, needs to be assessed in a randomized trial

This study has several limitations. First, most patients received chemotherapy before the start of radiotherapy and PET imaging. Chemotherapy can reduce the amount of tumor hypoxia and downregulates metabolism, resulting in a decreased uptake of HX4 and FDG (40). However, the focus of our research is on the correlation between both imaging modalities, therefore treatment differences between patients are less relevant. In addition, it is most important to have recent PET information before the start of (adaptive) radiotherapy. Second, we were not able to validate the current imaging observations on tumor specimens. Nevertheless, van Baardwijk et al. (41) showed previously that FDG-PET imaging is correlated to GLUT-1 and HIF-1α expression in NSCLC patients and Dubois et al. (8) showed a high correlation between HX4 PET uptake and pimonidazole staining in a rat rhabdomyosarcoma model. Third, the study acquired PET scans in free-breathing, which might cause blurring of the PET signal. Although, since both the FDG and HX4 scans were obtained in this setting, we do not expect any substantial bias for the comparison. Furthermore, advanced stage tumors are known to show little breathing induced motion (42, 43). Fourth, the FDG PET/CT was rigidly registered to the HX4 PET/CT scan to compare spatial uptake patterns. Small errors in registration can have a significant effect on correlation (44). However, patients in the current study were aligned in radiotherapy treatment position providing a strong basis for accurate registration. Fifth, there was a small time interval between the FDG and HX4 PET/CT scan. Changes in anatomy, tumor metabolism or hypoxia may have occurred in this interval and influenced the comparison results. The time interval in our study was short (median: 3 days) and no interventions (e.g. chemotherapy or radiotherapy) were performed between the two scans, limiting the chances of anatomical or physiological changes. Finally, the usability of a tracer for radiation dose-painting is dependent on its spatial reproducibility. Aerts et al. (45) showed that the location of low and high FDG volumes were stable during radiotherapy. The short time reproducibility for HX4 (2h vs. 4h) was confirmed, but the long term reproducibility is still unknown (6). However, a high reproducibility has been reported by Busk et al. (46) and Okamoto et al. (47) for the alternative hypoxia tracers FMISO and FAZA.

In conclusion, there is a positive correlation between GTV, FDG and HX4 uptake parameters on a tumor level. The hypoxic tumor volume is on average three times smaller than the metabolic active tumor volume. Approximately half of the lesions showed a good spatial correlation between the PET tracers. In the other cases, a (partial) mismatch was observed. Hypoxia PET imaging gives complimentary information to metabolic FDG imaging, which can potentially be used to individualize patient treatment by selecting patients for treatment with hypoxic sensitizers or hypoxia PET based radiotherapy dose escalation.

## Supplementary Material

Refer to Web version on PubMed Central for supplementary material.

## Acknowledgments

**Financial support:** National Institute of Health (NIH-USA U01 CA 143062-01, Radiomics of NSCLC), the CTMM framework (AIRFORCE project, grant 030-103), the EU 6th and 7th framework program (METOXIA, EURECA, ARTFORCE), euroCAT (IVA Interreg - www.eurocat.info), and the Kankeronderzoekfonds Limburg of the Health Foundation Limburg and the Dutch Cancer Society (KWF UM 2011-5020, KWF UM 2009-4454, KWF MAC 2011-4970, KWF MAC 2013-6425).

The authors would like to thank the patients who agreed to participate, C. Overhof for handling the data-management for both clinical trials and R. Franssen for the data acquisition. We acknowledge financial support from the National Institute of Health (NIH-USA U01 CA 143062-01, Radiomics of NSCLC), the CTMM framework (AIRFORCE project, grant 030-103), the EU 6th and 7th framework program (METOXIA, EURECA, ARTFORCE), euroCAT (IVA Interreg - www.eurocat.info), and the Kankeronderzoekfonds Limburg of the Health Foundation Limburg and the Dutch Cancer Society (KWF UM 2011-5020, KWF UM 2009-4454, KWF MAC 2011-4970, KWF MAC 2013-6425).

## References

1. Siegel R, Naishadham D, Jemal A. Cancer statistics, 2013. CA Cancer J Clin. 2013; 63:11–30. [PubMed: 23335087]
2. Auperin A, Le Pechoux C, Rolland E, Curran WJ, Furuse K, Fournel P, et al. Meta-analysis of concomitant versus sequential radiochemotherapy in locally advanced non-small-cell lung cancer. J Clin Oncol. 2010; 28:2181–90. [PubMed: 20351327]
3. Nordsmark M, Bentzen SM, Rudat V, Brizel D, Lartigau E, Stadler P, et al. Prognostic value of tumor oxygenation in 397 head and neck tumors after primary radiation therapy. An international multi-center study. Radiother Oncol. 2005; 77:18–24. [PubMed: 16098619]
4. Zips D, Zophel K, Abolmaali N, Perrin R, Abramyuk A, Haase R, et al. Exploratory prospective trial of hypoxia-specific PET imaging during radiochemotherapy in patients with locally advanced head-and-neck cancer. Radiother Oncol. 2012; 105:21–8. [PubMed: 23022173]
5. Milosevic M, Warde P, Menard C, Chung P, Toi A, Ishkanian A, et al. Tumor hypoxia predicts biochemical failure following radiotherapy for clinically localized prostate cancer. Clin Cancer Res. 2012; 18:2108–14. [PubMed: 22465832]
6. Zegers CM, van Elmpt W, Wierts R, Reymen B, Sharifi H, Ollers MC, et al. Hypoxia imaging with [(18)F]HX4 PET in NSCLC patients: Defining optimal imaging parameters. Radiother Oncol. 2013; 109:58–64. [PubMed: 24044790]
7. Bollineni VR, Kerner GS, Pruim J, Steenbakkers RJ, Wiegman EM, Koole MJ, et al. PET Imaging of Tumor Hypoxia Using 18F-Fluoroazomycin Arabinoside in Stage III-IV Non-Small Cell Lung Cancer Patients. J Nucl Med. 2013
8. Dubois LJ, Lieuwes NG, Janssen MH, Peeters WJ, Windhorst AD, Walsh JC, et al. Preclinical evaluation and validation of [18F]HX4, a promising hypoxia marker for PET imaging. Proc Natl Acad Sci U S A. 2011; 108:14620–5. [PubMed: 21873245]
9. van Loon J, Janssen MH, Ollers M, Aerts HJ, Dubois L, Hochstenbag M, et al. PET imaging of hypoxia using [18F]HX4: a phase I trial. Eur J Nucl Med Mol Imaging. 2010; 37:1663–8. [PubMed: 20369236]
10. Chen L, Zhang Z, Kolb HC, Walsh JC, Zhang J, Guan Y. (1)(8)F-HX4 hypoxia imaging with PET/CT in head and neck cancer: a comparison with (1)(8)F-FMISO. Nucl Med Commun. 2012; 33:1096–102. [PubMed: 22836736]
11. Aerts HJ, van Baardwijk AA, Petit SF, Offermann C, Loon J, Houben R, et al. Identification of residual metabolic-active areas within individual NSCLC tumours using a pre-radiotherapy (18)Fluorodeoxyglucose-PET-CT scan. Radiother Oncol. 2009; 91:386–92. [PubMed: 19329207]

12. Abramyuk A, Tokalov S, Zophel K, Koch A, Szluha Lazanyi K, Gillham C, et al. Is pre-therapeutical FDG-PET/CT capable to detect high risk tumor subvolumes responsible for local failure in non-small cell lung cancer? Radiother Oncol. 2009; 91:399–404. [PubMed: 19168248]
13. Spijkerman J, Fontanarosa D, Das M, van Elmpt W. Validation of nonrigid registration in pretreatment and follow-up PET/CT scans for quantification of tumor residue in lung cancer patients. 2014
14. Lambin P, van Stiphout RG, Starmans MH, Rios-Velazquez E, Nalbantov G, Aerts HJ, et al. Predicting outcomes in radiation oncology--multifactorial decision support systems. Nat Rev Clin Oncol. 2013; 10:27–40. [PubMed: 23165123]
15. Aerts HJ, Lambin P, Ruysscher DD. FDG for dose painting: a rational choice. Radiother Oncol. 2010; 97:163–4. [PubMed: 20561697]
16. Lambin P, Petit SF, Aerts HJ, van Elmpt WJ, Oberije CJ, Starmans MH, et al. The ESTRO Breur Lecture 2009. From population to voxel-based radiotherapy: exploiting intra-tumour and intra-organ heterogeneity for advanced treatment of non-small cell lung cancer. Radiother Oncol. 2010; 96:145–52. [PubMed: 20647155]
17. Pereira KM, Chaves FN, Viana TS, Carvalho FS, Costa FW, Alves AP, et al. Oxygen metabolism in oral cancer: HIF and GLUTs (Review). Oncol Lett. 2013; 6:311–6. [PubMed: 24137322]
18. van Elmpt W, De Ruysscher D, van der Salm A, Lakeman A, van der Stoep J, Emans D, et al. The PET-boost randomised phase II dose-escalation trial in non-small cell lung cancer. Radiother Oncol. 2012; 104:67–71. [PubMed: 22483675]
19. Doss M, Zhang JJ, Belanger MJ, Stubbs JB, Hostetler ED, Alpaugh K, et al. Biodistribution and radiation dosimetry of the hypoxia marker 18F-HX4 in monkeys and humans determined by using whole-body PET/CT. Nucl Med Commun. 2010; 31:1016–24. [PubMed: 20948452]
20. Boellaard R, Oyen WJ, Hoekstra CJ, Hoekstra OS, Visser EP, Willemsen AT, et al. The Netherlands protocol for standardisation and quantification of FDG whole body PET studies in multi-centre trials. European journal of nuclear medicine and molecular imaging. 2008; 35:2320–33. [PubMed: 18704407]
21. Cherk MH, Foo SS, Poon AM, Knight SR, Murone C, Papenfuss AT, et al. Lack of correlation of hypoxic cell fraction and angiogenesis with glucose metabolic rate in non-small cell lung cancer assessed by 18F-Fluoromisonidazole and 18F-FDG PET. J Nucl Med. 2006; 47:1921–6. [PubMed: 17138734]
22. Vera P, Bohn P, Edet-Sanson A, Salles A, Hapdey S, Gardin I, et al. Simultaneous positron emission tomography (PET) assessment of metabolism with (1)(8)F-fluoro-2-deoxy-d-glucose (FDG), proliferation with (1)(8)F-fluoro-thymidine (FLT), and hypoxia with (1)(8)fluoro-misonidazole (F-miso) before and during radiotherapy in patients with non-small-cell lung cancer (NSCLC): a pilot study. Radiother Oncol. 2011; 98:109–16. [PubMed: 21056487]
23. Gagel B, Piroth M, Pinkawa M, Reinartz P, Zimny M, Kaiser HJ, et al. pO polarography, contrast enhanced color duplex sonography (CDS), [18F] fluoromisonidazole and [18F] fluorodeoxyglucose positron emission tomography: validated methods for the evaluation of therapy-relevant tumor oxygenation or only bricks in the puzzle of tumor hypoxia? BMC Cancer. 2007; 7:113. [PubMed: 17598907]
24. Cistaro A, Quartuccio N, Mojtahedi A, Fania P, Filosso PL, Campenni A, et al. Prediction of 2 years-survival in patients with stage I and II non-small cell lung cancer utilizing (18)F-FDG PET/CT SUV quantification. Radiol Oncol. 2013; 47:219–23. [PubMed: 24133385]
25. Tanaka H, Hayashi S, Hoshi H. Pretreatment maximum standardized uptake value on 18F-fluorodeoxyglucose positron emission tomography is a predictor of outcome for stage I non-small cell lung cancer after stereotactic body radiotherapy. Asia Pac J Clin Oncol. 2013
26. Satoh Y, Onishi H, Nambu A, Araki T. Volume-based parameters measured by using FDG PET/CT in patients with stage I NSCLC treated with stereotactic body radiation therapy: prognostic value. Radiology. 2014; 270:275–81. [PubMed: 24029640]
27. Eschmann SM, Paulsen F, Reimold M, Dittmann H, Welz S, Reischl G, et al. Prognostic impact of hypoxia imaging with 18F-misonidazole PET in non-small cell lung cancer and head and neck cancer before radiotherapy. J Nucl Med. 2005; 46:253–60. [PubMed: 15695784]

28. Overgaard J. Hypoxic modification of radiotherapy in squamous cell carcinoma of the head and neck--a systematic review and meta-analysis. Radiother Oncol. 2011; 100:22–32. [PubMed: 21511351]
29. Arrieta O, Blake M, de la Mata-Moya MD, Corona F, Turcott J, Orta D, et al. Phase II study. Concurrent chemotherapy and radiotherapy with nitroglycerin in locally advanced non-small cell lung cancer. Radiother Oncol. 2014; 111:311–5. [PubMed: 24836861]
30. Saggar JK, Tannock IF. Activity of the hypoxia-activated pro-drug TH-302 in hypoxic and perivascular regions of solid tumors and its potential to enhance therapeutic effects of chemotherapy. Int J Cancer. 2014; 134:2726–34. [PubMed: 24338277]
31. Lohith TG, Kudo T, Demura Y, Umeda Y, Kiyono Y, Fujibayashi Y, et al. Pathophysiologic correlation between 62Cu-ATSM and 18F-FDG in lung cancer. J Nucl Med. 2009; 50:1948–53. [PubMed: 19910425]
32. Moller DS, Khalil AA, Knap MM, Muren LP, Hoffmann L. A planning study of radiotherapy dose escalation of PET-active tumour volumes in non-small cell lung cancer patients. Acta Oncol. 2011; 50:883–8. [PubMed: 21767188]
33. Vander Heiden MG, Cantley LC, Thompson CB. Understanding the Warburg effect: the metabolic requirements of cell proliferation. Science. 2009; 324:1029–33. [PubMed: 19460998]
34. Dang CV, Le A, Gao P. MYC-induced cancer cell energy metabolism and therapeutic opportunities. Clin Cancer Res. 2009; 15:6479–83. [PubMed: 19861459]
35. Dubois L, Landuyt W, Haustermans K, Dupont P, Bormans G, Vermaelen P, et al. Evaluation of hypoxia in an experimental rat tumour model by [(18)F]fluoromisonidazole PET and immunohistochemistry. Br J Cancer. 2004; 91:1947–54. [PubMed: 15520822]
36. Rasey JS, Koh WJ, Evans ML, Peterson LM, Lewellen TK, Graham MM, et al. Quantifying regional hypoxia in human tumors with positron emission tomography of [18F]fluoromisonidazole: a pretherapy study of 37 patients. Int J Radiat Oncol Biol Phys. 1996; 36:417–28. [PubMed: 8892467]
37. Petit SF, Dekker AL, Seigneuric R, Murrer L, van Riel NA, Nordsmark M, et al. Intra-voxel heterogeneity influences the dose prescription for dose-painting with radiotherapy: a modelling study. Phys Med Biol. 2009; 54:2179–96. [PubMed: 19293465]
38. Thorwarth D, Eschmann SM, Paulsen F, Alber M. Hypoxia dose painting by numbers: a planning study. Int J Radiat Oncol Biol Phys. 2007; 68:291–300. [PubMed: 17448882]
39. Due AK, Vogelius IR, Aznar MC, Bentzen SM, Berthelsen AK, Korreman SS, et al. Recurrences after intensity modulated radiotherapy for head and neck squamous cell carcinoma more likely to originate from regions with high baseline [18F]-FDG uptake. Radiother Oncol. 2014; 111:360–5. [PubMed: 24993331]
40. Bittner MI, Wiedenmann N, Bucher S, Hentschel M, Mix M, Weber WA, et al. Exploratory geographical analysis of hypoxic subvolumes using 18F-MISO-PET imaging in patients with head and neck cancer in the course of primary chemoradiotherapy. Radiother Oncol. 2013; 108:511–6. [PubMed: 23849686]
41. van Baardwijk A, Dooms C, van Suylen RJ, Verbeken E, Hochstenbag M, Dehing-Oberije C, et al. The maximum uptake of (18)F-deoxyglucose on positron emission tomography scan correlates with survival, hypoxia inducible factor-1alpha and GLUT-1 in non-small cell lung cancer. Eur J Cancer. 2007; 43:1392–8. [PubMed: 17512190]
42. Bosmans G, van Baardwijk A, Dekker A, Ollers M, Boersma L, Minken A, et al. Intra-patient variability of tumor volume and tumor motion during conventionally fractionated radiotherapy for locally advanced non-small-cell lung cancer: a prospective clinical study. Int J Radiat Oncol Biol Phys. 2006; 66:748–53. [PubMed: 17011450]
43. Yu ZH, Lin SH, Balter P, Zhang L, Dong L. A comparison of tumor motion characteristics between early stage and locally advanced stage lung cancers. Radiother Oncol. 2012; 104:33–8. [PubMed: 22677039]
44. Nyflot MJ, Harari PM, Yip S, Perlman SB, Jeraj R. Correlation of PET images of metabolism, proliferation and hypoxia to characterize tumor phenotype in patients with cancer of the oropharynx. Radiother Oncol. 2012; 105:36–40. [PubMed: 23068711]

45. Aerts HJ, Bosmans G, van Baardwijk AA, Dekker AL, Oellers MC, Lambin P, et al. Stability of 18F-deoxyglucose uptake locations within tumor during radiotherapy for NSCLC: a prospective study. Int J Radiat Oncol Biol Phys. 2008; 71:1402–7. [PubMed: 18234432]

46. Busk M, Mortensen LS, Nordsmark M, Overgaard J, Jakobsen S, Hansen KV, et al. PET hypoxia imaging with FAZA: reproducibility at baseline and during fractionated radiotherapy in tumour-bearing mice. European journal of nuclear medicine and molecular imaging. 2013; 40:186–97. [PubMed: 23076620]

47. Okamoto S, Shiga T, Yasuda K, Ito YM, Magota K, Kasai K, et al. High reproducibility of tumor hypoxia evaluated by 18F-fluoromisonidazole PET for head and neck cancer. J Nucl Med. 2013; 54:201–7. [PubMed: 23321456]

## Statement of translational relevance

The ultimate goal of cancer treatment is to provide patient-specific treatment based on tumor characteristics. High tumor metabolism and hypoxia are known to cause treatment resistance. Non-invasive imaging of tumor metabolism (FDG-PET) is already frequently performed in standard clinical practice, but imaging of tumor hypoxia (HX4-PET) is still in the clinical research stage. Both modalities provide the opportunity to show tumor characteristics in 3D, which can be used for response prediction and treatment adaptation. Radiotherapy dose-painting based on FDG-PET imaging, for example, is already performed in clinical trials. HX4-PET imaging might provide complimentary information to FDG-PET; we therefore performed an extensive comparison of the two imaging modalities. This study shows a (partial) spatial mismatch between FDG and HX4-PET imaging in some NSCLC tumors. The addition of HX4-PET imaging in treatment adaptation might therefore have the potential to individualize patient treatment and improve loco-regional control.

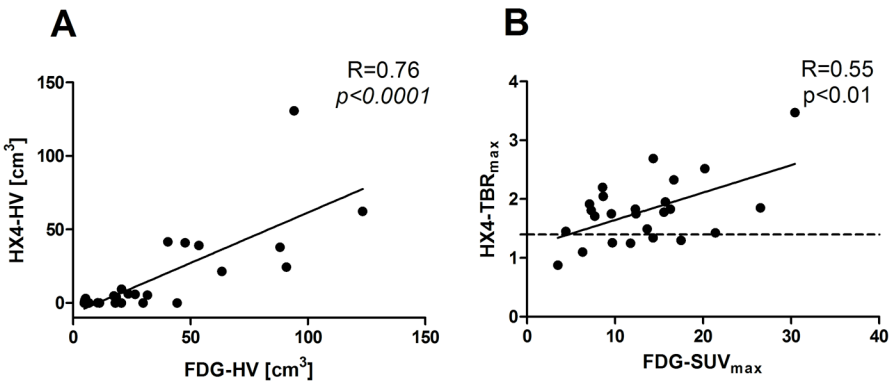


**Figure 1.**

Comparison between FDG and HX4 PET based parameters: A: FDG high volume versus HX4 high volume and B: FDG-$SUV_{max}$ versus HX4-TBR, the dashed line shows the threshold to define hypoxia (HX4-$TBR_{max}$ = 1.4).

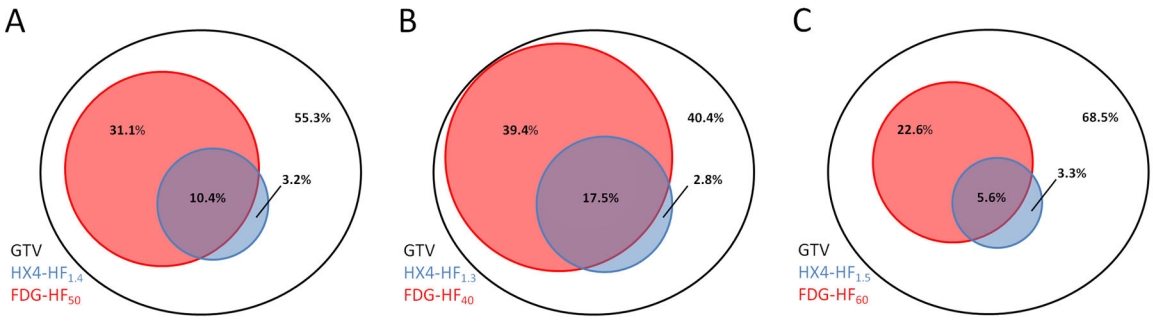


**Figure 2.**

Visualization of the overlap between FDG and HX4 high fraction (HF). A: Using the standard thresholds TBR>1.4 (HX4) and SUV>50%$SUV_{max}$ (FDG), B: Using alternative thresholds TBR>1.3 (HX4) and SUV>40% of $SUV_{max}$ (FDG), and C: Using the alternative thresholds TBR>1.5 (HX4) and SUV>60% of $SUV_{max}$ (FDG).

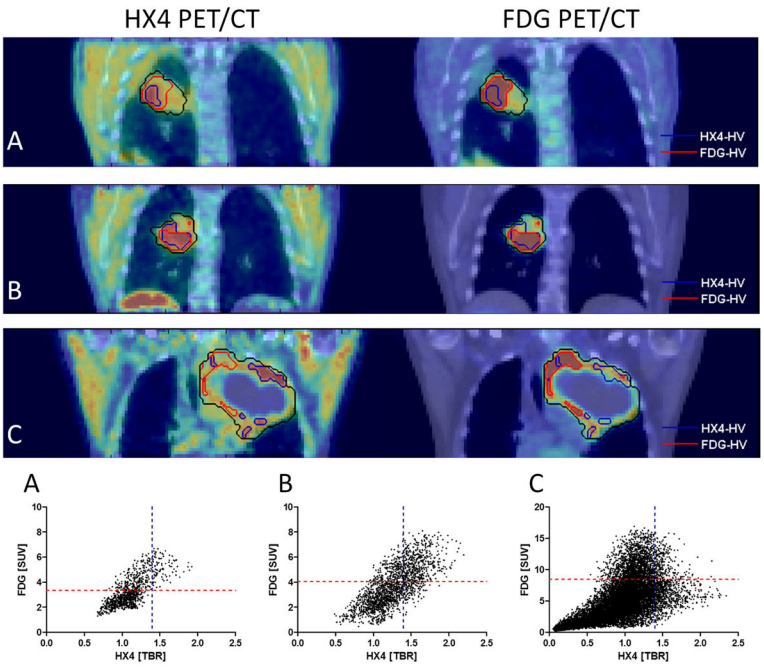


**Figure 3.**

Visual and voxel-wise comparison of HX4 and FDG PET/CT. A: HX4 high volume (HX4-HV) within the FDG high volume (FDG-HV), B: Partial overlap between HX4-HV and FDG-HV, C: Two distinct uptake patterns.

**Table 1**

FDG- and HX4-uptake parameters (mean±SD) for the primary lesions (GTVprim) and involved lymph nodes (GTVln).

| | N | Volume GTV | FDG | | | | HX4 | | | | |
|---|---|---|---|---|---|---|---|---|---|---|---|
| | | | $SUV_{mean}$ | $SUV_{max}$ | HF | HV | $SUV_{mean}$ | $SUV_{max}$ | $TBR_{max}$ | HF | HV |
| **GTVprim** average (*range*) | 25 | 127±173 $cm^3$ *(6–852 $cm^3$)* | 5.3±2.5 *(1.7–10.9)* | 13.3±6.6 *(3.5–30.4)* | 41±21% *(10–85%)* | 36±33 $cm^3$ *(5–123 $cm^3$)* | 0.8±0.3 *(0.4–1.2)* | 1.3±0.4 *(0.6–2.1)* | 1.8±0.6 *(0.9–3.5)* | 14±15% *(0–49%)* | 18±30$cm^3$ *(0–131$cm^3$)* |
| **GTVln** average *(range)* | 19 | 57±72 $cm^3$ *(7–254$cm^3$)* | 3.9±1.5 *(1.3–6.7)* | 9.3±4.0 *(2.4–18.5)* | 49±22% *(20–92%)* | 29±40$cm^3$ *(2–139 $cm^3$)* | 0.7±0.2 *(0.4–1.0)* | 1.1±0.4 *(0.5–1.8)* | 1.7±0.5 *(1.1–2.8)* | 7±10% *(0–37%)* | 7±13$cm^3$ *(0–46$cm^3$)* |

**Table 2**

Pearson's correlation coefficient (R) and corresponding p-values of GTVprim based parameters on FDG and HX4 PET

| | **Volume GTVprim** | **HX4-SUV$_{mean}$** | **HX4-SUV$_{max}$** | **HX4-TBR$_{max}$** | **HX4-HF** | **HX4-HV** |
|---|---|---|---|---|---|---|
| Volume GTVprim | | | | | | |
| R | - | 0.16 | 0.48 | 0.49 | 0.01 | 0.60 |
| *p* | - | *0.48* | *0.02* | *0.01* | *0.95* | *<0.01* |
| FDG-SUV$_{mean}$ | | | | | | |
| R | 0.13 | 0.52 | 0.58 | 0.46 | 0.44 | 0.52 |
| *p* | *0.54* | *0.01* | *<0.01* | *0.02* | *0.03* | *<0.01* |
| FDG-SUV$_{max}$ | | | | | | |
| R | 0.47 | 0.39 | 0.54 | 0.55 | 0.28 | 0.66 |
| *p* | *0.02* | *0.07* | *<0.01* | *<0.01* | *0.17* | *<0.001* |
| FDG-HF | | | | | | |
| *R* | −0.47 | 0.20 | 0.02 | −0.14 | 0.31 | −0.18 |
| *P* | *0.02* | *0.36* | *0.93* | *0.49* | *0.13* | *0.40* |
| FDG-HV | | | | | | |
| *R* | 0.83 | 0.32 | 0.61 | 0.64 | 0.28 | 0.76 |
| *p* | *<0.0001* | *0.14* | *<0.01* | *<0.01* | *0.18* | *<0.0001* |

*Clin Cancer Res*. Author manuscript; available in PMC 2017 January 12.

**Table 3**

Average distribution of high and low HX4 and FDG uptake within the GTVprim. Standard thresholds were used: TBR>1.4 (HX4) and SUV>50%$SUV_{max}$ (FDG)

| Overlap between | FDG-low average *(range)* | FDG-high average *(range)* | GTV |
|---|---|---|---|
| HX4-low | (i) 55.3±21.9% *(8.5–89.8%)* | (ii) 31.1±19.5% *(9.8–84.3%)* | 86.4±15.5 *(50.7–100%)* |
| HX4-high | (iii) 3.2±6.5% *(0–31.0%)* | (iv) 10.4±12.2% *(0–43.4%)* | 13.6±15.5 *(0–49.3%)* |
| GTV | 58.5±21.6% *(14.6–89.8%)* | 41.5±21.2% *(10.2–85.4%)* | 100% |